Supporting Information: Electro-Hydrodynamic Extraction of DNA from mixtures of DNA and Bovine Serum Albumin

Benjamin E. Valley, Anne D. Crowell, Jason E. Butler, and Anthony J. C. Ladd*

Department of Chemical Engineering, University of Florida, Gainesville FL, U.S.A.

E-mail: tladd@che.ufl.edu

Device Fabrication

The device was fabricated by fusing polymethylmethacrylate (PMMA or acrylic; Astra Products) sheets in a thermal press.[1] First, two 200 micron thick and one 1/8 in thick, 1 in $\times$ 2 in sheets were cut using CO_2 laser ablation (Trotec-Speedy 360). An expansion–contraction pattern (Figure 1b of the main article) was cut into one of the thin sheets, and inlet, outlet, and sample injection ports were cut into the thick sheet. The three sheets were then cleaned with light detergent and 70 % (v/v) isopropyl alcohol (Santa Cruz Biotechnology). The sheets were stacked between two glass plates and thermally welded in a dual heat plate manual press (Color King, China) at 230°F for one hour, and were allowed to cool for 30 minutes before being removed from the press. Luer connectors (Nordson Plastics) were then attached to the inlet, outlet, and injection ports using epoxy. A rubber septum (Nordson Plastics) connected to the injection port enabled sample injection directly into the expansion section of the device, upstream of the channel. A photograph of the assembled device

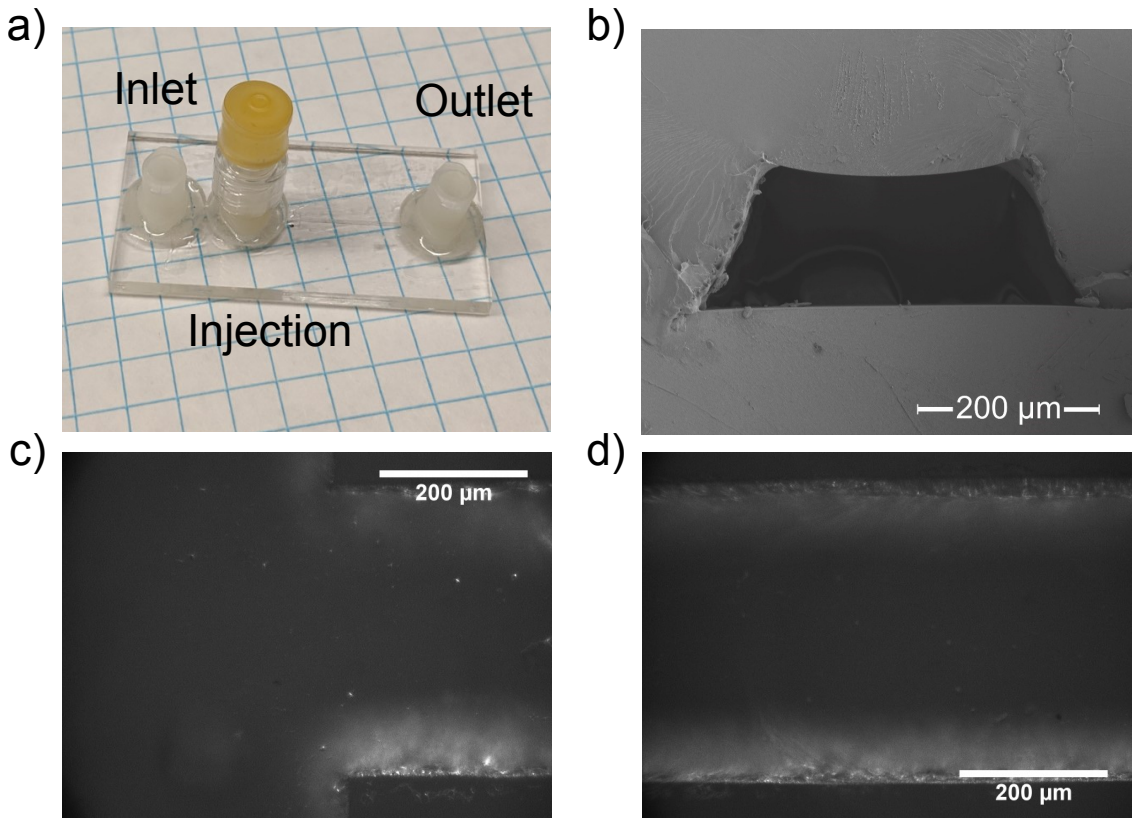

Figure 1: Images of the microfluidic device. (a) The assembled device showing the inlet, injection, and outlet ports. (b) Scanning electron micrograph (SEM) of a cross section of the contraction channel. (c) Brightfield micrograph of the channel entrance, corresponding to the solid red square in Figure 2b. (d) The exit region of the contraction channel, corresponding to the dashed red square in Figure 2c. The SEM images were provided by Mr. Sarathy Kannan Gopalakrishnan.

is shown in Figure 1a.

Channel features cut into PMMA sheets using CO_2 laser ablation yielded trapezoidal shaped channels (Figure 1b), consistent with other reports.[2–4] The minimum and maximum widths of the contraction channel were approximately 290 and 390 microns (average channel width of ≈ 340 μm). The average depth of the device was ≈ 150 μm. The height reduction from the 200 μm thickness of the original PMMA sheet is due to the pressure applied during the thermal bonding process.

Brightfield micrographs of portions of the device are shown in Figures 2b & c of the main article. Thirty two images were taken at different locations within the device with a Keyence BZ-X810 microscope (4x objective) and then stitched together using BZ-X Analyzer software. Higher resolution micrographs of the viewing areas (red squares in Figures 2b & c), taken with the Nikon Diaphot 200 camera, are shown in Figures 1c & d.

Solution and Sample Preparation

Buffer solution was prepared by diluting concentrated (100x) Tris-EDTA (TE) buffer (Sigma) with deionized water (Barnstead Nanopure, 18.2 MΩ·cm) to a standard 0.25x solution containing 2.5 mM Tris-HCl and 0.25 mM EDTA. Neutral polymer, polyvinylpyrrolidone (PVP), with a molecular weight of 40 kDa (Sigma), was added to a concentration of 0.5 % (w/w) to reduce electroosmosis towards the outlet. The buffer solution (pH $\approx$ 7.3) was then filtered (0.22 μm, PES) and degassed under vacuum for 30 minutes prior to use.

Diluted TE was chosen as the process buffer because it is commonly used for preservation of nucleic acids. The concentration of TE was reduced from those typically used for DNA storage to reduce the ionic strength (8 mM for 0.25x TE) of the flowing buffer solution.[5] Acrylic capillaries have an inherent electroosmotic flow (EOF), and PVP was selected to act as a dynamic channel coating because it is frequently used to eliminate EOF in glass capillaries.[6–8] Its use as a sieving matrix in capillary electrophoresis of DNA suggests it has

a minimal effect on the DNA and is not a PCR inhibitor.[9]

DNA-BSA mixtures were prepared by adding λ-DNA (New England Biolabs, 48 kbp) and BSA (Sigma, 66.5 kDa) at concentrations of 0.1 ng/μL and 30 mg/mL respectively, to a 0.25x TE buffer solution. The concentration of protein is similar to physiological concentrations, while the DNA concentration is roughly two orders of magnitude lower than those commonly encountered in blood samples.[10,11] The low concentration of DNA was used to test if the extraction method would function with samples containing small amounts of DNA (1 ng). BSA was chosen as a proxy for proteins in general, because albumin comprises the majority of serum proteins. Like DNA, it is negatively charged at a neutral pH.[10]

DNA-BSA mixtures were fluorescently tagged to quantify the concentration of DNA and BSA. YOYO-3 (1 mM stock solution in dimethyl sulfoxide, Invitrogen) DNA intercalating dye was used to label the DNA at a ratio of four base pairs to one dye molecule. BSA was tagged by mixing unlabeled BSA with FITC-BSA (Sigma) at a concentration of 2.5 % (w/w). YOYO-3 emits red light (612/631 nm excitation/emission) while FITC emits green light (494/520 nm). FITC-BSA was only used in experiments to measure BSA concentration; this eliminates interference with DNA quantification from the high levels of FITC-BSA fluorescence.

Calibrations

The acrylic channel was mounted into the experimental setup as indicated by the schematic in Figure 2a of the main article and the reservoirs were filled with approximately 40 mL of the process buffer. Fluid flow through the device was driven by a height difference between the two reservoirs. The flow rate was adjusted by lowering the height of the outlet reservoir using a translation stage (Thorlabs). The stage was adjusted by a stepper motor controlled by an open source microcontroller (Arduino Leonardo board). The centerline velocity of the fluid in the channel, v_0, was measured by tracking the displacement of fluorescent latex beads

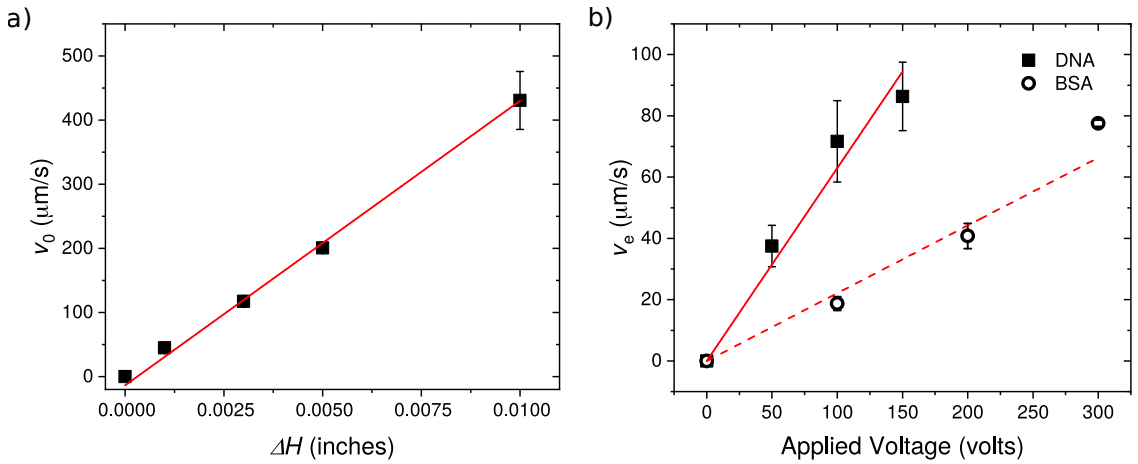

Figure 2: Velocity calibrations. The red lines are linear fits to the data; the error bars indicate one standard deviation. (a) Average centerline fluid velocity (v_0) ($n = 3$). (b) Average electrophoretic velocities (v_e) of DNA (black squares; $n = 3$) and BSA (open black circles; $n = 2$).

(PolyScience) as a function of height difference between the reservoirs. A linear correlation between centerline particle velocity and height difference was observed (Figure 2a) with a slope of 44 mm/s per inch height difference. This relation was used to control the fluid velocity in all the experiments; typical flow rates were on the order of 1 mL/hr ($v_0 = 1$ mm/s).

Electric fields in the device were generated by applying up to 250 volts across stainless steel electrodes placed in the reservoirs (Agilent 3321A voltage generator and Trek 2220 amplifier). The maximum field within the channel was about 140 V/cm, with nearly all the potential drop occurring within the 1.8 cm long contraction channel.[12] The electrophoretic velocity of DNA was measured by tracking the motion of individual, fluorescently tagged molecules. However, BSA molecules are too small to be tracked individually. Instead, the displacement of a slug of FITC-BSA was measured as a function of time. The electrophoretic velocities of DNA and BSA were found to be 0.6 μm/s per volt and 0.2 μm/s per volt respectively. Linear correlations between electrophoretic velocity and applied voltage are shown in Figure 2b.

Epifluorescence images were captured with a Nikon Diaphot 200 inverted microscope

equipped with a QImaging Retiga SRV CCD camera. All images were collected using a 200 ms exposure time and a gain of 39 unless stated otherwise. A Nikon ELWD 20x/0.4 objective was used for imaging. In epifluorescence mode, Nikon B-1A (blue) and Nikon G-1B (green) excitation filters were used to image FITC-BSA and YOYO-3, respectively. A mercury lamp (Nikon HB 10101AF) with an Osram HBO Mercury short-arc 103W/2 bulb was used to stimulate the fluorophores. Illumination of the device was controlled by a motorized shutter actuated by an open source microcontroller (Arduino Uno board). A custom MATLAB (MathWorks, 2014) based controller program was used to control all operations associated with the experiment, including shutter actuation, image acquisition, reservoir height difference, and applied voltage.

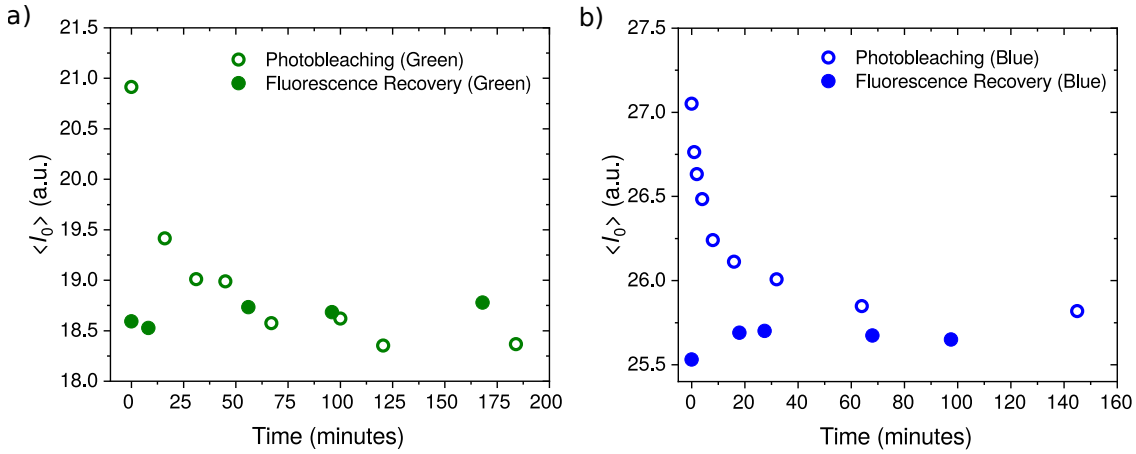

Figure 3: Baseline pixel intensity of the pure buffer solution $\langle I_0 \rangle$. The open circles show the decay of the autofluorescence of PMMA as a function of time under constant illumination. The solid circles show the extent of fluorescence recovery within 2–3 hours; the sample is illuminated for brief periods while the fluorescence is being measured. Images were taken at the channel entrance. (a) Green excitation filter. (b) Blue excitation filter.

Prior to an experiment or calibration, the selected viewing window was illuminated for 2 hours, to photobleach the region under observation. The average pixel intensity, $\langle I_0 \rangle$, is shown as a function of illumination time in Figure 3. Acrylic devices have high background signals due to PMMA's intrinsic autofluorescence, but irradiating the channel in advance of measurements quenches the autofluorescence signal (Figure 3).[13] While the intensity of PMMA's background signal does recover after photobleaching (Figure 3), it is at rates slow

enough that the recovery of the background signal can be neglected. The minimal values of $\langle I_0 \rangle$ are used as the baseline intensity in subsequent measurements. The shutter was left open during the rinse cycles between experiments to photobleach any fluorophores adsorbed to the walls and to further suppress the acrylic's autofluorescence signal.

The relationship between fluorescent intensity and concentration was calibrated by injecting approximately 20 μL of solution with known concentration directly into the device. The calibration solutions were convected past the field of view using a syringe pump (Harvard Apparatus) at a rate of approximately 0.9 mL/hr. The intensity of each solution, $\langle I \rangle$, was determined as an average over the same viewing window used in the later experiments, and corrected by subtracting off the average baseline intensity of the pure buffer solution, $\langle I^\star \rangle = \langle I \rangle - \langle I_0 \rangle$. Sample calibration curves for DNA and BSA are provided in Figures 4 and 5. The slopes of the calibration lines relating concentration of DNA (ng/μL) or FITC-BSA (mg/mL) to average fluorescent intensity, $C = \beta \langle I^\star \rangle$, were measured daily to account for degradation in the output of the mercury lamp.

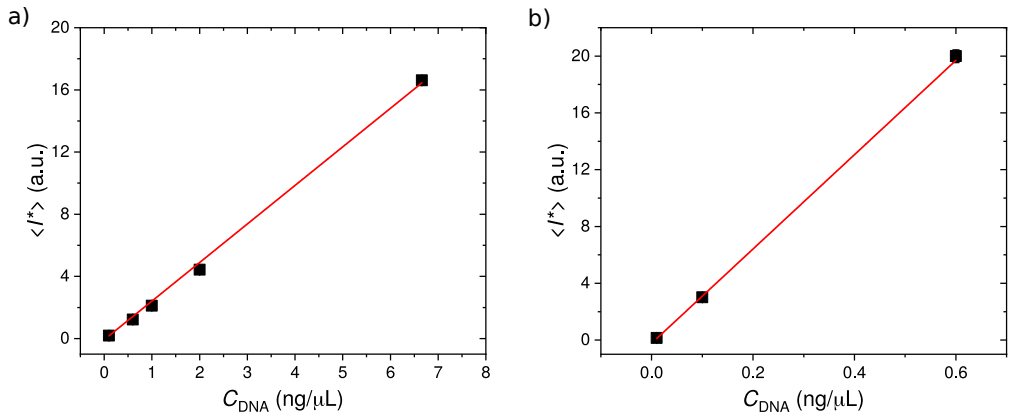

Figure 4: A DNA concentration calibration from the baseline-corrected intensity $\langle I^\star \rangle$ of samples of known concentration (ng/μL). (a) $\langle I^\star \rangle$ vs. DNA concentration at the contraction channel entrance. Data was acquired using the 8x neutral density filter and a gain setting of 30. (b) $\langle I^\star \rangle$ vs. DNA concentration near the contraction channel exit. Data was acquired without neutral density filtering and with a gain setting of 39. The solid red lines are linear fits of the data. The error bars (one standard deviation, $n = 2$) are smaller than the symbols.

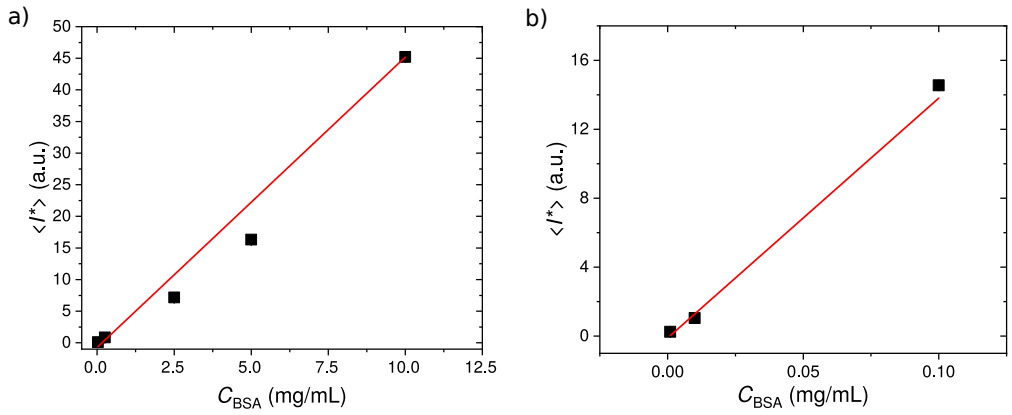

Figure 5: A BSA concentration calibration from the baseline-corrected intensity $\langle I^{\star} \rangle$ of samples of known concentration (mg/mL). (a) $\langle I^{\star} \rangle$ vs. BSA concentration at the contraction channel entrance. Data was acquired using the 8x neutral density filter and a gain setting of 30. (b) $\langle I^{\star} \rangle$ vs. BSA concentration near the contraction channel entrance. Data was acquired without neutral density filtering and with a gain setting of 39. The solid red lines are linear fits of the data. The error bars (one standard deviation, $n = 2$) are smaller than the symbols.

References

(1) Liga, A.; Morton, J. A. S.; Kersaudy-Kerhoas, M. *Microfluidics and Nanofluidics* **2016**, *20*, 164.

(2) Islam, M. M.; Loewen, A.; Allen, P. B. *Sci. Rep.* **2018**, *8*, 8763.

(3) Nayak, N. C.; Lam, Y. C.; Yue, C. Y.; Sinha, A. T. *J. Micromech. Microeng* **2008**, *18*, 095020.

(4) Cheng, J.-Y.; Wei, C.-W.; Hsu, K.-H.; Young, T.-H. *Sens. Actuators B Chem* **2004**, *99*, 186–196.

(5) Montes, R. J.; Ladd, A. J. C.; Butler, J. E. *Biomicrofluidics* **2019**, *13*, 044104.

(6) Ross, D.; Johnson, T. J.; Locascio, L. E. *Anal. Chem.* **2001**, *73*, 2509–2515.

(7) Milanova, D.; Chambers, R. D.; Bahga, S. S.; Santiago, J. G. *Electrophoresis* **2012**, *33*, 3259–3262.

(8) Kaneta, T.; Ueda, T.; Hata, K.; Imasaka, T. *J. Chromatogr. A.* **2006**, *1106*, 52–55.

(9) Gao, Q.; Yeung, E. S. *Anal. Chem.* **1998**, *70*, 1382–1388.

(10) Busher, J. T. In *Serum Albumin and Globulin*; K., W. H., D., H. W., J.W., H., Eds., 3rd ed.; Boston: Butterworths, 1990; Chapter 101, pp 497–499.

(11) Ivarsson, M.; Carlson, J. Extraction, Quantitation, and Evaluation of Function DNA from Various Sample Types. In *Methods in Biobanking, Methods in Molecular Biology*; Dillner, J., Ed.; Springer, 2011; Vol. 675, Chapter 14, pp 261–277.

(12) Arca, M.; Ladd, A. J. C.; Butler, J. E. *Soft Matter* **2016**, *12*, 6975–6984.

(13) Piruska, A.; Nikcevic, I.; Lee, S. H.; Ahn, C.; Heineman, W. R.; Limbach, P. A.; Seliskar, C. J. *Lab Chip* **2005**, *5*, 1348–1354.